Polymethoxyflavones from Gardenia oudiepe and semi-synthetic derivatives reduce nociception in mice: Evidence for the involvement of the MAPK pathway

Clément Daviaud, Christiane Adrielly Alves Ferraz, Mariana Gama E Silva, Edilson Beserra de Alencar Filho, Sammya Yasmin Evangelista Mendes de Lima, Vincent Dumontet, Lucindo José Quintans Júnior, Jackson Roberto Guedes da Silva Almeida, Laurent Picot, Kévin Baranger, et al.

Biomedicine & Pharmacotherapy 182 (2025) 117742

Contents lists available at ScienceDirect

Biomedicine & Pharmacotherapy

journal homepage: www.elsevier.com/locate/biopha

Polymethoxyflavones from *Gardenia oudiepe* and semi-synthetic derivatives reduce nociception in mice: Evidence for the involvement of the MAPK pathway

Clément Daviaud [a], Christiane Adrielly Alves Ferraz [b], Mariana Gama e Silva [c], Edilson Beserra de Alencar Filho [d], Sammya Yasmin Evangelista Mendes de Lima [d], Vincent Dumontet [e], Lucindo José Quintans Júnior [f], Jackson Roberto Guedes da Silva Almeida [g], Laurent Picot [a], Kévin Baranger [a], Raimundo Gonçalves de Oliveira Júnior [b,*], Raphaël Grougnet [b,*]

[a] UMRi CNRS 7266 LIENSs, Université de La Rochelle, La Rochelle 17042, France
[b] UMR CNRS 8038 CiTCoM, Université Paris Cité, Paris 75006, France
[c] Departamento de Ciências Biológicas (DCBIO), Universidade Estadual de Feira de Santana, Feira de Santana 44036-900, Brazil
[d] Colegiado de Ciências Farmacêuticas, Universidade Federal do Vale do São Francisco, Petrolina 56304-205, Brazil
[e] Laboratoire des Plantes Médicinales de Nouméa, CNRS-Centre IRD, BP 643, Nouméa Cedex, Nouvelle-Calédonie 98845, France
[f] LANEF, Universidade Federal de Sergipe, Aracaju 49100-000, Brazil
[g] NEPLAME, Universidade Federal do Vale do São Francisco, Petrolina 56304-205, Brazil

ARTICLE INFO

Keywords:
flavonoids
inflammation
nociception
medicinal plants
MAPK pathway

ABSTRACT

This study explores the potential of polymethoxyflavones (PMFs) and polyacetylated flavones (PAFs) as novel analgesic and anti-inflammatory agents. Eight derivatives, isolated from *Gardenia oudiepe* bud exudate or semi-synthesized from commercial kaempferol, underwent evaluations in various *in vivo*, *in vitro*, and *in silico* models. Acetic acid-, formalin-induced pain, and hot-plate tests were conducted in mice (n = 6). Cell viability assay, ELISA, NO measurement and protein expression by western blot were determined on RAW264.7 macrophage cells before and after exposure to LPS. Molecular docking was performed in order to putatively corroborate the affinity of the compound library to the most promising targets. Despite closely-related chemical structures, subtle modifications significantly influenced anti-nociceptive activity and affinity on diverse cellular or enzymatic targets. The library of compounds exhibited noticeable inhibitory effects on nociception in acetic acid- and formalin-induced pain assays in mice. Biochemical assays on RAW264.7 cells elucidated anti-inflammatory properties, highlighting PAFs **7** and **8** as the most active. The study indicates a peripheral anti-nociceptive profile, suggesting interferences with the production of inflammatory mediators implicated in pain disorders (*e.g.,* COX-2, Tnf-α, IL-6 and MAPK pathway proteins). Molecular docking analyses strongly suggested interactions between PMFs/PAFs chemical library and pre-selected targets. PAFs **7** and **8** demonstrated the best binding energies, showing potential in tackling inflammation, possibly by binding to MAPK, ERK, JNK and p38. These data provide insights for lead optimization through further pharmacomodulation, paving the way for the development of innovative multi-target analgesic and anti-inflammatory drugs.

Abbreviations: AU, arbitrary units; COX-2, cyclooxygenase-2; DMSO, dimethyl sulfoxide; ERK, extracellular signal regulated kinase; IB, immunoblot; INDO, indomethacin; JNK, c-Jun N-terminal kinase; MAPK, mitogen-activated protein kinase; MOR, morphine; NO, nitric oxide; Ns, non-significant; OD, optical density; PAF, polyacetylated flavone; PMF, polymethoxyflavone; RMSD, root mean square deviations; SAR, structure-activity relationships.

* Corresponding authors.
E-mail addresses: raimundo.goncalves-de-oliveira-junior@u-paris.fr (R.G. de Oliveira Júnior), raphael.grougnet@u-paris.fr (R. Grougnet).

https://doi.org/10.1016/j.biopha.2024.117742
Received 23 August 2024; Received in revised form 4 December 2024; Accepted 8 December 2024
Available online 12 December 2024

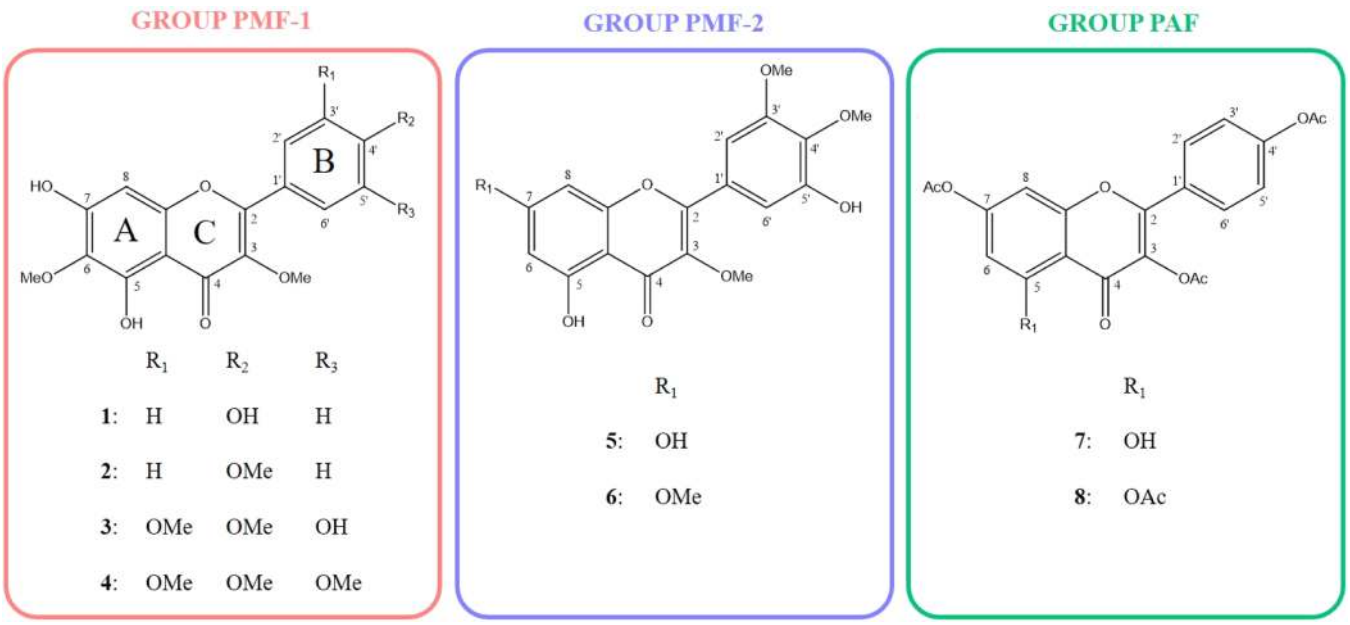

Fig. 1. Structures of PMFs and PAFs Flavonoids from *Gardenia oudiepe* and semisynthetic derivatives of kaempferol. The carbon atoms are numbered (2–8, 1'-6') and the rings are identified (A-C). **1–8** were pooled in 3 groups (PMF-1, PMF-2, PAF) to better compare their pharmacological effects.

1. Introduction

Pain is a consequence of pathophysiological processes involved in several chronic and acute disorders, playing an important role in the detection of tissue damage and activation of repair signaling pathways [1]. Despite being also an emotional and subjective experience, previous investigations have described neurobiological mechanisms for pain transduction, transmission and modulation. During injuries, nociceptors are activated by chemical, thermal or mechanical agents, inducing the release of neurogenic and inflammatory mediators that sensitize nociceptive fibers and contribute to the amplification of noxious stimuli [2–4]. Due to its complexity, pain management usually includes the use of analgesic and/or anti-inflammatory drugs, according to the clinical condition. However, central and peripheral analgesics are frequently associated with strong and potentially detrimental side effects, such as dependence, respiratory depression, gastrointestinal and renal lesions [5–8]. Consequently, the search for safe and efficient analgesic and anti-inflammatory agents appears as a major public health priority, aiming to relieve acute and chronic pain in the context of aging population.

Over the last decades, many pharmacological studies have described the antinociceptive potential of flavones. Indeed, these metabolites isolated from food or medicinal plants, can act on targets involved in central (opioids, adrenergic, dopaminergic, GABAergic receptors) and peripheral (COX, histamine, bradykinin, pro-inflammatory cytokines) pain pathways [9–12]. Furthermore, numerous investigations involving natural and/or semisynthetic polymethoxyflavones (PMFs) and polyacetylated flavones (PAFs) aiming to explore structure-activity relationships (SAR) have led to the main noticeable conclusion: despite of closely-related chemical structures, minor differences (such as the replacement of a phenol with a methoxyle group) dramatically influence the level of selectivity and specificity towards cellular or enzymatic targets (*e.g.,* tyrosinase and xanthine oxidase) and thus their mechanisms of action [13–15].

In this context and to further demonstrate the potential of PMFs and PAFs as bioactive compounds, eight derivatives (Fig. 1) were evaluated for inhibition of nociception in several animal models. The library of PMFs was mainly built from bud exudate, a renewable part of *Gardenia oudiepe* (syn. *G. cerifera*), a non-endangered small tree endemic to New Caledonia. This raw material is easy to harvest and its collection in small amounts from each plant does not damage the specimen. Moreover, it is simple to work with, as it does not require any step of extraction. Dissolution using a minimum volume of low-polar organic solvent followed by paper filtration and evaporation under reduced pressure provide a gum, ready for chromatographic separations. Flavones **1-6** were isolated and then characterized after comparison with literature data. In order to extend the library of derivatives, acetylation of commercial kaempferol was performed and has led to **7** and **8**, depending on the reaction conditions [13]. Compounds **1-8** were evaluated *in vivo* in three different pain models using as positive controls the well-known antinociceptive drugs morphine (MOR) and indomethacin (INDO). Biochemical assays *in vitro* were then carried out in order to deepen the analyses of their anti-inflammatory properties and to identify some targets. Furthermore, a virtual molecular docking using *in silico* approaches was performed, aiming to propose putative interactions of the compounds with proteins involved in peripheral nociception and inflammation.

2. Material and methods

2.1. Plant material

Bud exudates of *G. oudiepe* Vieill. were collected and identified by one of us (V.D.) in Forêt Plate, North Province of New Caledonia (October 2008). A voucher specimen is kept at the Herbarium of the Botanical and Tropical Ecology Department of the IRD Center, Noumea, New Caledonia (reference POU-0290).

2.2. Isolation of flavones 1–6 from G. oudiepe

Bud exudates of *G. oudiepe* (200 g) were dissolved in 1 L of dichloromethane. After filtration through a Buchner funnel and evaporation of the solvent under reduced pressure, 52.0 g of exudates free from vegetal pieces were recovered. Chromatographic separations on normal phase silica gel using solvents mixtures of increasing polarity cyclohexane/dichloromethane and dichloromethane/methanol as eluent provided compounds **1-6**. ^{1}H and ^{13}C NMR data of all flavones were in accordance with those previously reported [13,14].

2.3. Semi-synthesis of flavones 7 and 8 from kaempferol

The triacetyl-kaempferol **7** was semi-synthetized by stirring commercial kaempferol (80 mg, 0.28 mmol, Sigma-Aldrich®) for 15 min at room temperature with acetic anhydride in dried pyridine. Crudes were then submitted to precipitation and washing with iced water, followed by recrystallization in CH_2Cl_2/CH_3OH (9/1, v/v) to provide 108 mg (0.26 mmol) of **7** (yield: 95 %). When the same protocol was applied to commercial kaempferol (80 mg) for 4 h, the tetraacetyl derivative **8** was obtained (120 mg, 0.26 mmol, yield: 95 %), as previously described [13, 14].

2.4. Antinociceptive activity

2.4.1. Animals and ethics statement

The experiments were carried out using 8-weak-old male Swiss mice (*Mus musculus*) (30–40 g). The animals were randomly housed in appropriate cages (six per group) at 22 ± 2 °C on a 12 h light/dark cycle (lights on at 7:00 a.m.) with free access to food (Purina Labina®) and water. They were allowed to have a period of acclimation (48 h) before any experimental protocol. The same visual observers (RGOJ, MGS and CAAF) conducted all pharmacological tests. This study was performed in accordance with the *Conselho Nacional para o Controle de Experimentação Animal* (CONCEA, Brazil) and complied with the recommendations of the International Association for the Study of Pain (IASP) [16]. All experimental procedures were approved by the Comitê de Ética no Uso de Animais from the Universidade Federal do Vale do São Francisco (CEUA-UNIVASF) with authorization number 0003/060916.

2.4.2. Drug treatments

The animals were divided in groups (n = 6) and submitted to different treatments. The negative control group was treated with the vehicle used for **1**-**8** and for the solubilization of the standard drugs (0.9 % saline solution, containing 10 μL Tween 80, 10 ml/kg). Compounds **1**-**8** were administrated orally (10 mg/kg, similar or lower dose than the standard drugs) 60 min before all behavioral analysis. Morphine (10 mg/kg) and indomethacin (20 mg/kg) were used as positive controls, administrated intraperitoneally (i.p.) 30 or 60 min before behavioral analysis, according to the protocol.

2.4.3. Acetic-acid-writhing-induced nociception

The writhing test was used as a classic model in order to assess the antinociceptive activity of the flavones, according to the protocol previously described[17], with some adaptations. The mice (n = 6) were treated with vehicle (10 ml/kg, p.o.), **1**-**8** (10 mg/kg, p.o.), morphine (10 mg/kg, i.p.) or indomethacin (20 mg/kg, i.p.). After 30 (for standard drugs) or 60 min (for negative control and **1**-**8** groups), the animals received 10 ml/kg (i.p.) of a 0.9 % acetic acid solution and the number of abdominal writhing was recorded during 10 min, beginning 5 min after acetic acid injection. Writhing was defined as a contraction of the abdominal wall, pelvic rotation followed by hind limb extension.

2.4.4. Formalin-induced nociception

The formalin test was conducted as previously described [18], with some adaptations. The animals (n = 6) were treated with vehicle (10 ml/kg, p.o.), flavones **1**-**8** (10 mg/kg, p.o.), morphine (10 mg/kg, i.p.) or indomethacin (20 mg/kg, i.p.) 60 min before the injection of a 2.5 % formalin solution (diluted in 0.9 % saline) into the right hind paw (20 μl/paw, subplantar). They were then observed in chambers with a mirror mounted on three sides and the time (in s) spent licking or biting the injected paw was measured as an indicator of pain. Behavioral responses were measured for 0–5 min (first phase, neurogenic pain) and 15–30 min (second phase, inflammatory pain) after the formalin injection.

2.4.5. Hot plate test

The hot plate test was performed in order to investigate the antinociceptive effect of the flavone derivatives in mice submitted to thermal stimulus. The animals were submitted to a pre-selection 24 h before the experiments: they were placed on a hot plate apparatus (Insight®, Brazil) at 55 ± 0.5°C; those showing a reaction time (defined as the latency for licking the hind feet or jumping) greater than 20 s were excluded from the study. The selected animals were treated with vehicle (10 ml/kg, p.o.), flavones **1**-**8** (10 mg/kg, p.o.) or morphine (10 mg/kg, i.p.). Latency time was recorded for each animal on the hot plate (55 °C) during a maximum period of 20 s, at intervals of 30, 60, 90 and 120 min after treatments.

2.5. Cell culture

2.5.1. ELISA and cell viability

DMEM, Penicillin/streptomycin (P/S) and Alamar Blue were purchased from Thermo Fischer Scientific (Villebon-Sur-Yvette, France). Fetal Bovine Serum (FBS) was from Dutscher (Brumath, France). LPS O55:B5 and dimethyl sulfoxide (DMSO) were purchased from Sigma-Aldrich (Saint-Quentin Fallavier, France). Murine macrophages RAW264.7 cells were cultivated in DMEM containing 10 % decomplemented and filtered FBS and 1 % P/S, as described and adapted from [19,20]. 1.8×10^5 cells/well, 500 μL/well in 24-well plates were plated for 24 h. Then, the cells were treated with LPS (1 μg/ml) with or without drugs at 10 μM for 24 h in DMEM containing 1 % P/S. The equivalent amount of DMSO was used as control. Supernatants were recovered and levels of Tnf-α and Il-6 were evaluated using ELISA from Peprotech (Neuilly-sur-Seine, France) according to manufacturer's recommendations. New warmed media (500 μL) DMEM, 1 % P/S containing 33 % Alamar Blue (Thermo Fischer Scientific) was added on each well for 2 h. Then, the absorbance was measured at 570 and 600 nm. The cell viability was expressed as the ratio of the values obtained at 570 and 600 nm for each condition. Absorbance were read using a spectrophotometer FluoroStar Omega (BMG LABTECH, Champigny-sur Marne, France).

2.5.2. NO measurement

RAW264.7 cells were cultivated in DMEM containing 10 % FBS and 1 % P/S and plated at 1.5×10^5 cells/well (100 μL) in 96-well plates for 24 h. Then, the cells were treated with LPS (1 μg/ml) with or without drugs at 10 μM for 24 h in DMEM containing 1 % P/S. The equivalent amount of DMSO was used as control. NO production was evaluated using Griess reagent according to manufacturer's recommendations (Thermo Fisher Scientific). Absorbance were read using a spectrophotometer FluoroStar Omega (BMG LABTECH, Champigny-sur Marne, France).

2.5.3. Western blot

Murine macrophages RAW264.7 cells were cultivated in DMEM containing 10 % decomplemented and filtered FBS and 1 % P/S. 3×10^5 cells/well/500 μL in 12-well plates were plated for 24 h. Then, the cells were treated with LPS (1 μg/ml) with or without drugs at 10 μM for 24 h in DMEM containing 1 % P/S. The equivalent amount of DMSO was used as control.

Protein concentration was measured using a Bio-Rad DC™ protein assay kit (Bio-Rad, Marnes-La-Coquette, France) and 30 μg of protein were loaded and run onto 4–20 % precast SDS-PAGE gels (Bio-Rad) and transferred to nitrocellulose membranes using the transblot rapid transfer system (Bio-Rad). The membranes were stained with Ponceau and then blocked with 5 % half-fat milk solution (w/v) for 1 h in Tris Buffered Saline containing 0.1 % Tween 20 (TBS-T, Sigma-Aldrich) at room temperature and probed overnight at 4 °C with the following primary antibodies against COX-2 (#4842, cyclooxygenase-2, Cell Signaling) and tubulin (1/3000, Abcam, Paris, France). Inflammatory pathways downstream TLR4 activation [21] were analyzed using p38

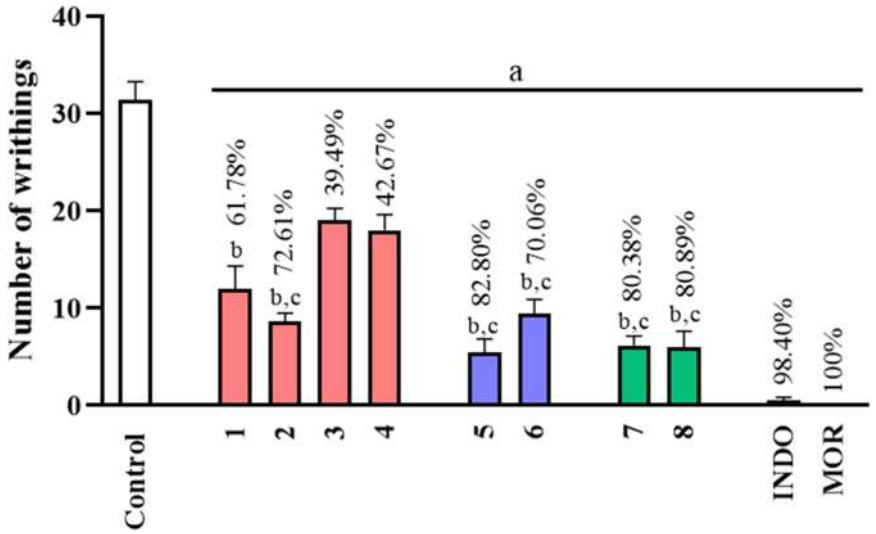

Fig. 2. Effect of flavones **1–8** (10 mg/kg, p.o.), indomethacin (INDO 20 mg/kg, i.p.) and morphine (MOR 10 mg/kg, i.p.) in acetic-acid-writhing-induced nociception test in mice (n = 6). Values are expressed as mean ± SEM, where [a,b,c] indicate $p < 0.05$, significantly different from the control group (vehicle), **3** and **4**, respectively, according to ANOVA, followed by Bonferroni's post-test. Groups are highlighted in red (PMF-1), blue (PMF-2) and green (PAF). The percentage of antinociceptive activity (mean %) is indicated above the corresponding column.

(#9212)/pP38 (#9211), ERK (#9107, extracellular signal-regulated kinase)/pERK (#9106), JNK (#9252, c-Jun N-terminal kinase)/pJNK (#4671) were purchased from Cell Signaling (Ozyme, Saint-Cyr-L'Ecole, France). Then, after washes with TBS-T, the membranes were incubated with horseradish peroxidase-conjugated secondary antibody (1/2000, Thermo Fisher Scientific). The immunoreactive bands were visualized using the ECL *Prime Western Blotting Reagent* (Bio-Rad) and a Chemidoc MP™ apparatus. Pictures were quantified using Fiji/ImageJ software (NIH). All the optical density plots represent normalized values to tubulin, as indicated in the figure legends.

2.6. Molecular docking studies

Molecular docking is a computational tool widely used to provide elucidations about the pharmacodynamics behavior of bioactive compounds [22]. Considering the small ligand/receptor systems, this method consists in the application of "search algorithms" combined with potential energy equations ("score functions") to get the best conformations of the small molecules on specific binding sites of macromolecules [22]. In this work, the Lamarkian Genetic Algorithm, implemented on Autodock v4.2 program (Autodock, Autogrid, Autotors, Copyright-1991–2000) from the Scripps Research Institute, http://www.scripps.edu/mb/olson/doc/autodock, was chosen to investigate the possible interactions profiles of the flavone derivatives. Initially, the PDB structures of the targets: p38, MAPK, ERK, JNK and COX-2 were obtained from the RCSB Protein Data Bank (https://www.rcsb.org/) with the codes 3S3I; 2ZOQ; 3V3V and 1CX2, respectively. All the proteins contained a co-crystallized ligand, including a flavonoid compound complexed with JNK. Proteins and original ligands were edited on Chimera 1.3 software [23]. Redocking [24] was made on each complex, using the "long mode" of the genetic algorithm [25,26], which corresponds to a maximum of the 25,000,000 energy evaluations during this procedure. Maximum number of generations was 27,000. The "grid box" was defined as centered on the center of the original ligands, with default box dimensions 40 × 40 × 40 Å, with spacing between grid points of 0.375 Å. The autodock "map types" were pre-calculated using the "autogrid" executable, considering the atomic parameters based on each ligand, for the force field calculations. These configurations provided good RMSD values (Root Mean Square Deviations) for all redockings (less than 2.0 Å), being then used to the dockings of the eight flavone derivatives. Hydrogens were added to all valences of the ligands using the Chimera. By default, only polar hydrogens were considered during the Autodock run, which are present in the generated images. The molecules were subjected to a previous geometry optimization at the semi-empirical PM3 level before the docking calculations [27].

2.7. Statistical analysis

All the results are presented as mean ± standard error of the mean (SEM) and statistical analyses were performed using one-way analysis of variance (ANOVA) followed by *post hoc* Dunnett's or Bonferroni's test, according to the experimental conditions. Values of $p < 0.05$ were considered statistically significant. All the analyses were performed using GraphPad Prism 6.0 software (GraphPad Prism Software, Inc., San Diego, CA, USA).

3. Results and discussion

3.1. Antinociceptive activity

Compounds **1**-**8** were evaluated for antinociceptive activity on several animal models. Initially, the acetic-acid-writhing-induced nociception test was performed with flavones at the dose of 10 mg/kg (p.o.), using the positive controls indomethacin (INDO) and morphine (MOR) at 20 and 10 mg/kg (i.p.) respectively (Fig. 2). It is a well-known and validated experimental model for the screening of new analgesic drugs [17]. As expected, INDO and MOR both exhibited strong antinociceptive effects (Fig. 2).

Few papers describe the correlation of the hydroxyl and methoxyl substitution pattern on the flavone core with the antinociceptive and anti-inflammatory activities. However, it has already been reported that hydroxyl groups on C-5 and C-7 (Fig. 1) together with the double bond Δ^{2-3} on the C-ring seem to be essential for a strong pharmacological efficacy [28,29].

All of the compounds significantly reduced the number of writhing after acetic acid injection (Fig. 2). Indeed, Flavones **5**, **7** and **8** were the most active, as they reduced pain behavior by 80–83 % compared to vehicle treated group; **1**, **2** and **6** exhibited an antinociceptive activity of 62–70 %, while **3** and **4** were the less promising derivatives ($p < 0.05$). According to these results, some structure-activity relationships may be proposed.

Flavones **1**-**4** with a methoxyl group on C-6 (A ring) are generally less

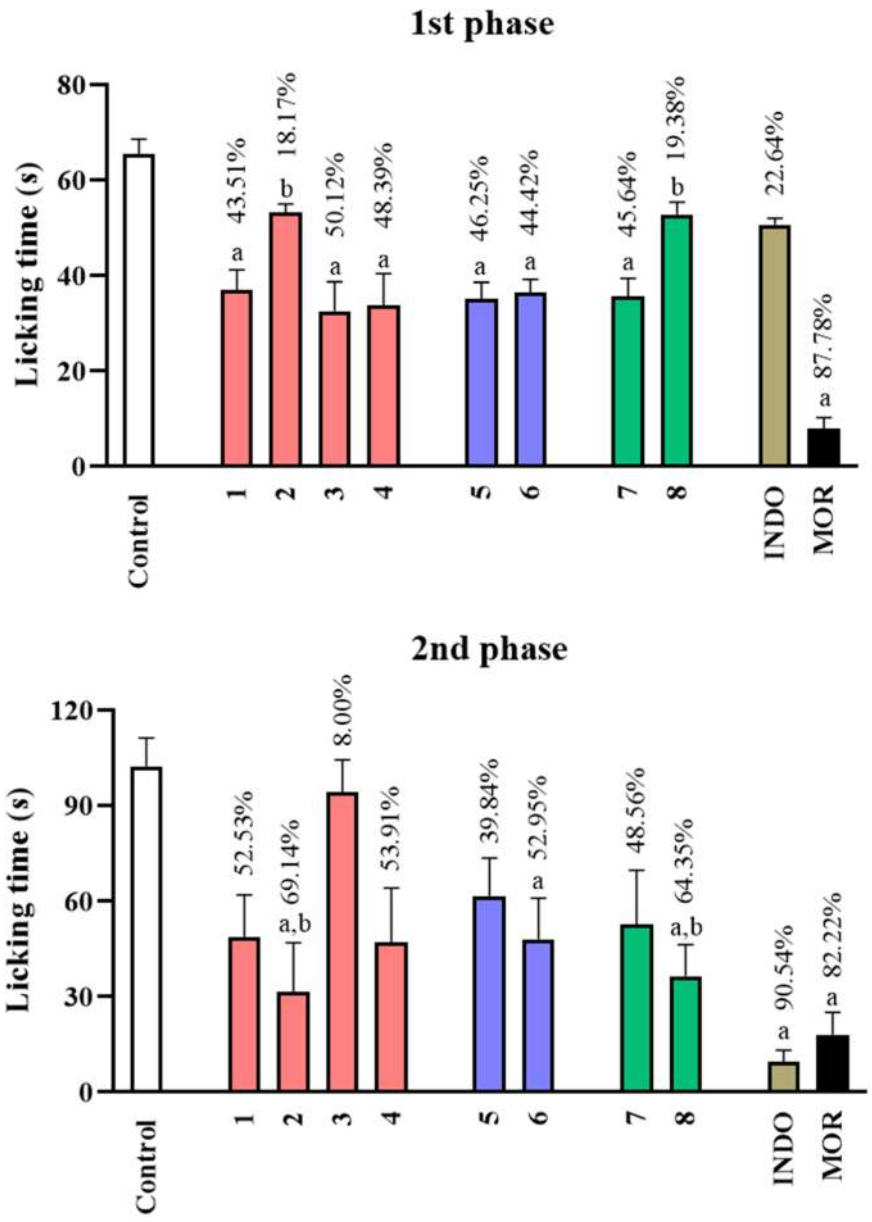

Fig. 3. Effect of flavones **1–8** (10 mg/kg, p.o.), indomethacin (INDO 20 mg/kg, i.p.) and morphine (MOR 10 mg/kg, i.p.) in the formalin-induced nociception test in mice (n = 6). Values are expressed as mean ± SEM, where [a,b] indicate $p < 0.05$, significantly different from the control group (vehicle) and **3**, respectively, according to ANOVA, followed by *post hoc* Bonferroni's test. Groups are highlighted in red (PMF-1), blue (PMF-2) and green (PAF). The percentage of antinociceptive activity (mean %) is described above the corresponding column.

active than **5-8**, which bear a hydrogen on this position. Nevertheless, **1** and **2**, with a low-hindered B-ring, remain quite efficient. Compounds **3**, **5** and **6** possess the same substitution pattern on B and C rings. In this scheme, **5** with only two hydroxyls on C-5 and C-7 is the most efficient with 82.80 % of antinociceptive effect. Methoxylation of C-7 in compound **6** leads to a slight decrease of the activity (70.06 %), which dramatically drops to 39.49 % in the case of **3** with an additional methoxyl group on C-6. PAFs **7** and **8** both strongly reduced nociception in a similar manner, suggesting that the acetylation of the phenol in position C-5 does not play an important role. Thus, these results suggested that a hydrogen, ie a low hindered group, on C-6 is probably fundamental for the activity.

Although all of the flavones demonstrated moderate to strong activity in the acetic-acid-writhing-induced nociception test, clear SAR remain difficult to highlight, as manifold molecular mechanisms are into play. Indeed, acetic acid injection sensitizes nociceptors located in the peritoneal region and stimulates the release of several painful and inflammatory mediators such as histamine, bradykinin, prostaglandins, substance P, serotonin, nitric oxide, glutamate, and noradrenaline [17]. Some of those are involved in fast-acting neurogenic responses (*e.g.,* serotonin, noradrenaline, glutamate), others in inflammatory processes (*e.g.,* histamine, bradykinin, prostaglandins). In this context, in order to determine in which signaling pathways the compounds effectively interfere with, we decided to perform the formalin-induced nociception and the hot plate tests.

The formalin-induced nociception test consists of two different phases: the first one (neurogenic pain) composed of a nociceptive response elicited by central-acting mediators, immediately after formalin subplantar injection and the second one (inflammatory pain) with predominance of inflammatory mediators, typically initiated 10–15 min after the pain stimulus [18]

Flavones **1** and **3-7** were moderately active during the first phase

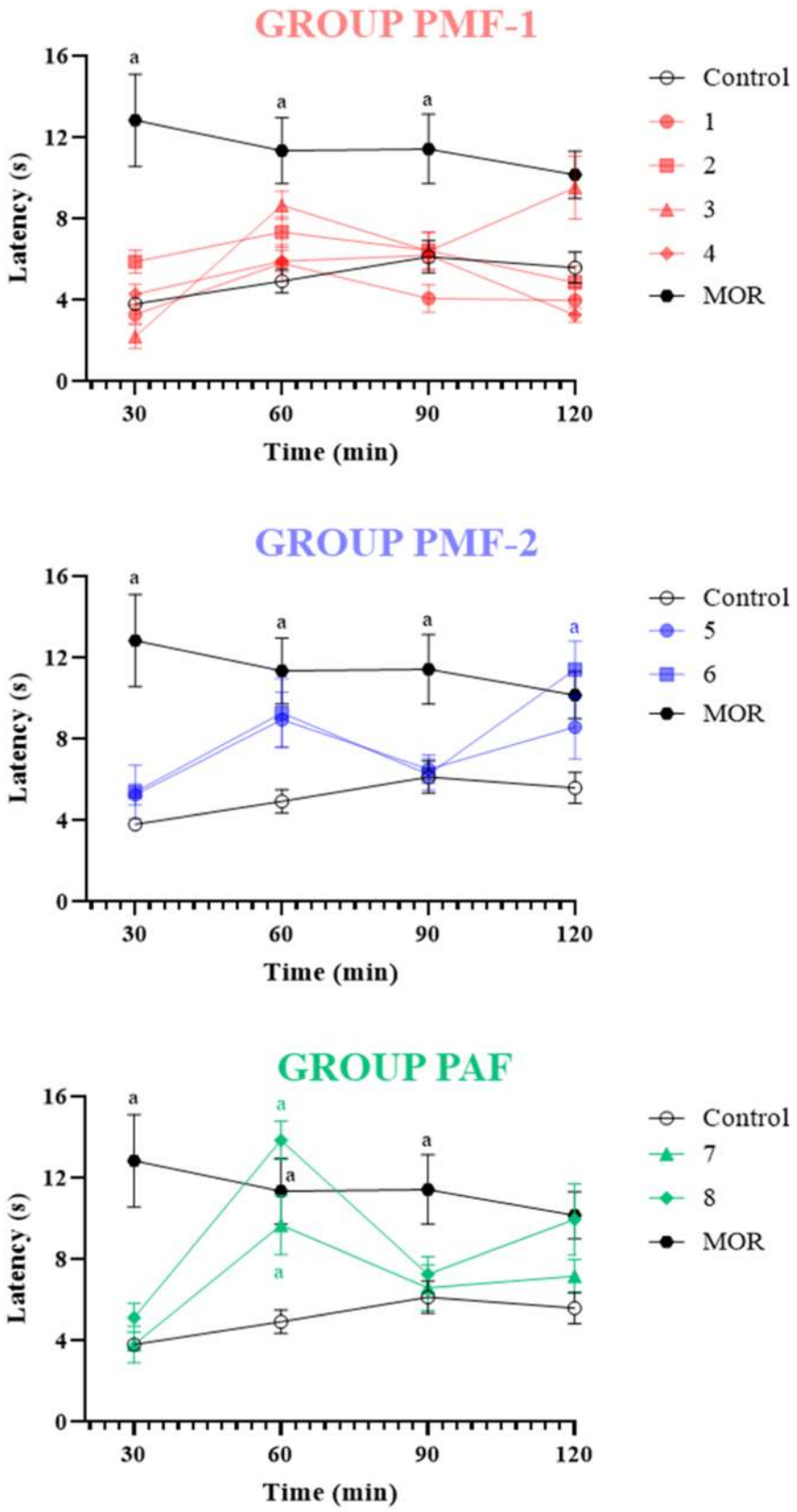

Fig. 4. Effect of flavones **1–8** (10 mg/kg, p.o.) and morphine (MOR 10 mg/kg, i.p.) in the hot plate test in mice (n = 6). Values are expressed as mean ± SEM, where [a] indicates $p < 0.05$, significantly different from the control group (vehicle), according to ANOVA, followed by *post hoc* Dunnett's test. Groups are highlighted in red (PMF-1), blue (PMF-2) and green (PAF).

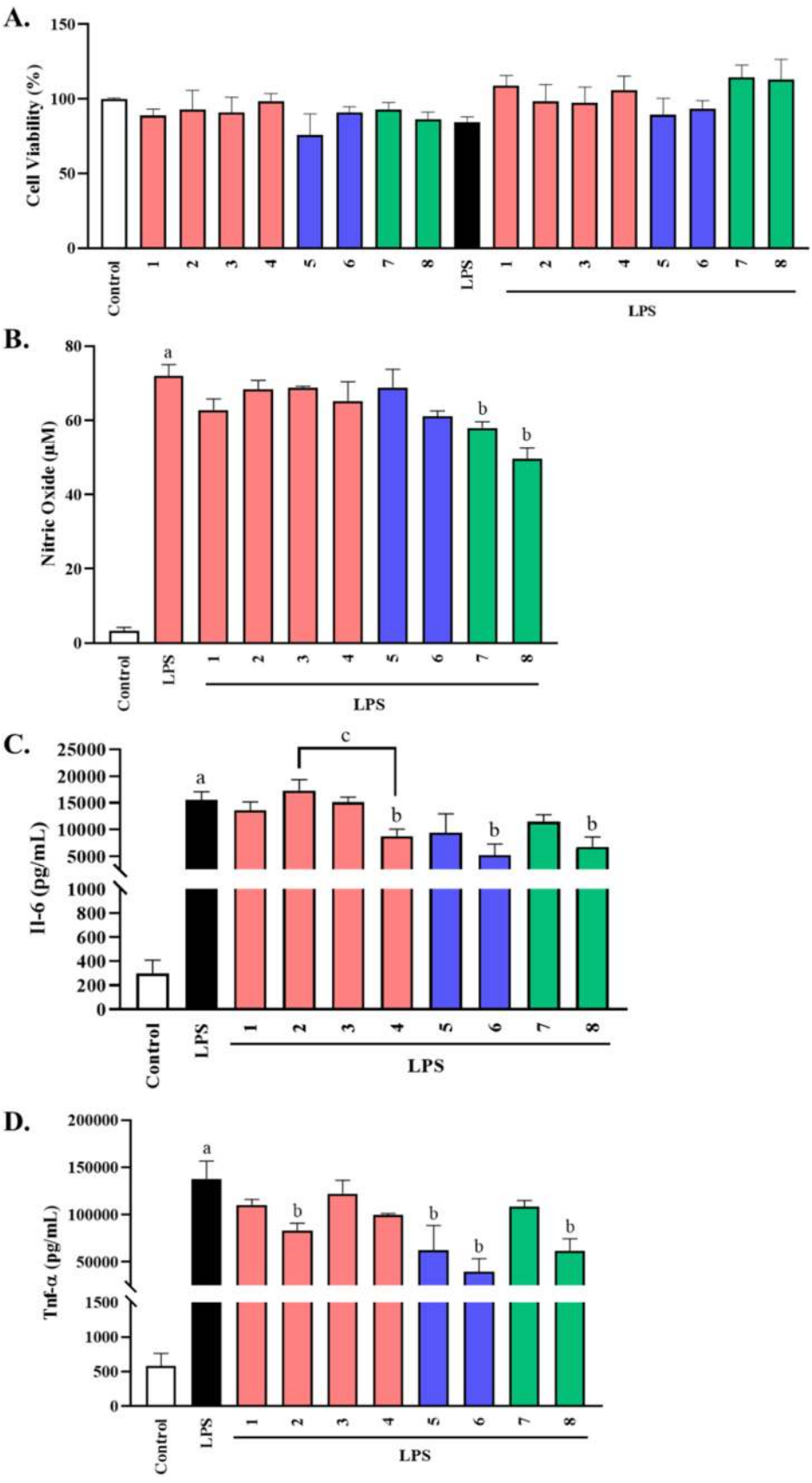

(caption on next page)

Fig. 5. Effect of molecules **1**-**8** on RAW264.7 cells viability, NO and cytokines production. Histograms showing the quantification of cell viability using the Alamar Blue assay (A), nitric oxide levels (B), Il-6 (C) and Tnf-α (D) levels measured by ELISA. White and black bars represent control and LPS (1 μg/ml for 24 h) condition, respectively. Groups are highlighted in red (PMF-1), blue (PMF-2) and green (PAF). Values are expressed as mean ± SEM from at least 3 independent cultures. [a,b,c] indicate $p < 0.05$, significantly different from the control, LPS or between tested molecules (**2** vs. **4**), respectively, according to ANOVA, followed by *post hoc* Bonferroni's test.

(Fig. 3) but compounds **2** and **8** exhibited low antinociceptive activity compared to vehicle administration. During the second phase, while **1**, **4**, **6** and **7** remained similarly active (although no significative difference was observed *vs.* control group, $p > 0.05$), **2** and **8** demonstrated a stronger antinociceptive effect than during the first phase (Fig. 3). Furthermore, a thorough analysis of the results highlights the opposite behavior of compounds **2** and **8** compared to **3** ($p < 0.05$). Indeed, **2** and **8** which were the less effective during the first phase, became the most active during the second phase, similar to the anti-inflammatory drug indomethacin (used as positive control) whereas **3**, the most active derivative at the beginning totally lost its efficiency during the second phase, suggesting that it probably targets different pathological

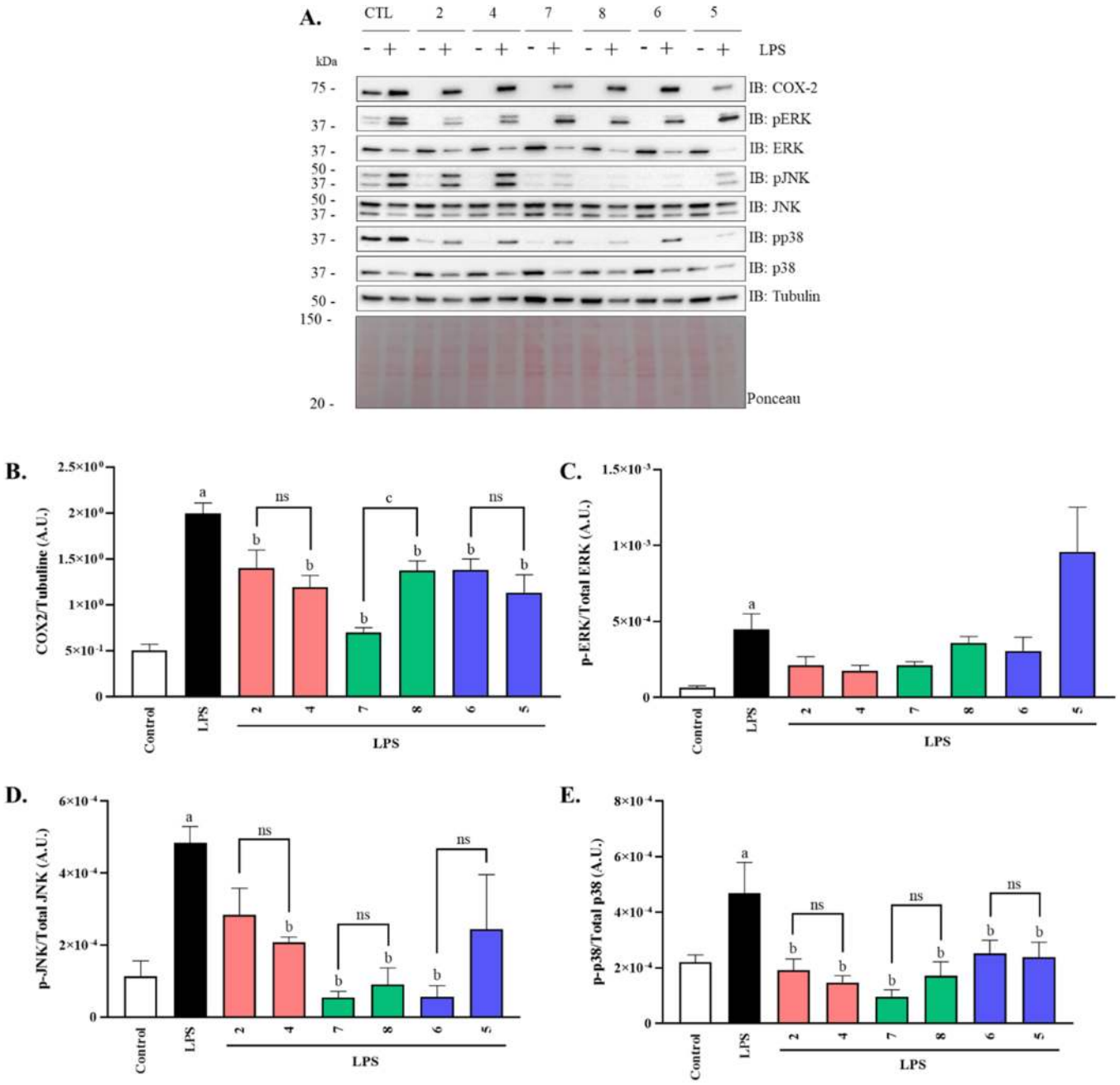

Fig. 6. Effects of **2**, **4**, **5**-**8** on MAPK signaling pathways. WB showing representative COX-2, pERK, ERK, pJNK, JNK, pp38, p38, tubulin signals and ponceau staining of the membrane (A) and the representative tubulin-normalized quantifications of COX-2 and pERK/ERK, pJNK/JNK, pp38/p38 ratios (B-E). White and black bars represent control and LPS (1 μg/ml for 24 h) condition, respectively. Groups are highlighted in red (PMF-1), blue (PMF-2) and green (PAF). Values are expressed as mean ± SEM from at least 3 independent cultures. [a,b,c] indicate $p < 0.05$, significantly different from the control, LPS or between tested molecules (**7** vs. **8**), respectively, according to ANOVA, followed by *post hoc* Bonferroni's test. IB: immunoblot. OD: optical density. A.U: arbitrary units. ns: non-significant.

Table 1
Binding Energies (Kcal/mol) and RMSD values from docking procedures.

Compound	MAPK		ERK		JNK		COX-2	
	BE*	RMSD*	BE	RMSD	BE	RMSD	BE	RMSD
0*	−10.55	1.22	−5.83	1.17	−7.54	0.87	−10.83	1.58
1	−7.14	-	−6.93	-	−7.19	-	−8.62	-
2	−7.15	-	−7.2	-	−6.78	-	−8.87	-
3	−8.09	-	−6.8	-	−7.31	-	−8.97	-
4	−7.79	-	−6.83	-	−7.04	-	−8.94	-
5	−6.71	-	−6.23	-	−8.2	-	−8.72	-
6	−8.63	-	−6.55	-	−7.97	-	−7.79	-
7	**−9.24**	-	**−8.34**	-	**−8.53**	-	**−9.97**	-
8	**−8.44**	-	**−8.47**	-	**−8.55**	-	**−10.18**	-

* 0 corresponds to the co-crystallized ligands in each receptor.

mechanisms.

Subsequently, the hot plate test was performed in order to further explore the involvement of central mechanisms in the antinociceptive effect of **1**-**8**. In this model, the animals have been submitted to a thermal stimulus, triggering the activation of neurogenic pathways (*e.g.,* vanilloid, glutamatergic, serotoninergic receptors, etc.). Only compounds **6**-**8** exhibited a significant antinociceptive response at 60 and 120 min (Fig. 4). It has to be noted that compound **3** exhibited a sigmoidal response *i.e.,* no effect at 30 and 90 min but positive effects compared to vehicle conditions. Overall, the combination of all of the data indicates that the pharmacological response induced by these flavones mostly involves the modulation of inflammatory pathways. This is supported by the lack of strong evidence for a central analgesic response in the hot-plate test, which is typically indicative of central nervous system involvement. Therefore, the observed effects (*e.g.,* second phase of the formalin test, Fig. 2) are more likely attributed to peripheral mechanisms associated with inflammation modulation.

Recently, antipyretic actions of viscosine (**1**) have been demonstrated *in vivo* mainly through interactions with mPGES1, and secondly with COX-1 and COX-2 [30]. Moreover, santin (**2**) has been described to attenuate the inflammation triggered by Influenza A virus infection by modulating p38 MAPK, JNK/SAPK, ERK, and NF-κB factor activities [31]. Both **1** and **2** were isolated from a fraction of *Heterotheca subaxillaris* (Asteraceae) which exhibited a strong *in vivo* anti-inflammatory activity (91 % of inhibition) in TPA (12-O-tetradecanoyl phorbol acetate)-induced ear edema test [32]. Compounds **3**-**6** are of rare occurrence and were evaluated in this work for the first time for their antinociceptive potential. Moreover, to the best of our knowledge, this is the first report of biological evaluation of PAFs **7** and **8** in the field of nociception and/or inflammation. For these reasons, in-depth *in vitro* pharmacology assays and molecular docking studies were performed with typical targets associated with the inflammatory processes.

3.2. Effect of PMFs and PAFs on inflammatory signaling pathways

Plausible mechanisms responsible for the antinociceptive activity of flavonoids have already been extensively reviewed; these compounds mostly interfere with various pro-inflammatory mediators produced by cells, depending on their subclass [33]. In addition to previous comments concerning viscosine (**1**) and santin (**2**), a recent work has demonstrated using *in vitro* and *in silico* experiments that the flavonol rhamnetin exerts its anti-inflammatory effect by triggering p38, ERK and JNK, members of the MAPK pathway [34], but also COX-2 levels, in LPS- or IFN-γ-stimulated RAW264.7 cells [35]. Considering that our library is made of 3-methoxyl or 3-acetyl-flavonol derivatives, the molecular targets cited above were considered as appropriate starting points for initial investigations about putative pharmacodynamic profiles.

In order to evaluate the putative anti-inflammatory properties of PMFs and PAFs, RAW264.7 murine cell macrophages model and LPS as trigger of inflammatory response were used. First, the absence of any cytotoxicity was checked using Alamar Blue assay. Compared to control condition, only **5** induced a 25 % but non-significative decrease of cell viability (Fig. 5A). LPS (1 μg/ml) treatment did not induce a significant cell stress in our conditions and none of the compounds exhibited toxicity upon LPS treatment (Fig. 5A).

The nitric oxide (NO) production was then measured using Griess reagent assay. At basal level, low amounts of NO were detected, which were not affected by any compounds (data not shown). As expected, LPS treatment markedly induced NO production and release over 70 μM. In these conditions, co-treatment with **1–6** did not alleviate NO levels while flavones **7** and **8** significantly dropped them to 58 and 49 μM, *i.e.,* by 20 and 31 %, respectively (Fig. 5B). These results were further confirmed by analyzing Il-6 and Tnf-α production by ELISA. The levels of these two pro-inflammatory cytokines were low in control conditions with no effects of our compounds (data not shown). As expected, LPS dramatically induced the release of these mediators (Fig. 5C and D).

Only compounds **4**, **6** and **8** significantly reduced Il-6 levels by 43, 66 and 57 %, respectively (Fig. 5C). Moreover, **4** significantly alleviated Il-6 levels compared to **2** by 51 %, suggesting the importance of the tri-OMe substitution pattern on the B-ring (Fig. 1).

Considering Tnf-α levels, **6** was the most efficient with a reduction of 71 %, while **2**, **5** and **8** were also significantly active (reduction of 39.7, 55 and 55 %, respectively, Fig. 5D).

To sum up, **6** was the most active compounds in both cases, followed by **8**. The latter was much more efficient than **7** underlining the major role of the additional acetylation on position 5. Flavone **4** only reduced Il-6 production, while 2 and 5 only interfered with the secretion of Tnf-α.

Aiming to deepen the analysis, the effects of **2** and **4–8** together were evaluated on COX-2 level, a well-known marker of inflammation, and on inflammatory kinases activation by western blot. Compunds **1** and **3** with no apparent anti-inflammatory activities within our conditions were not included in this step.

The six compounds dramatically reduced levels of COX-2, in unstimulated control conditions (Fig. 6A and B). Upon LPS treatment, levels of COX-2 were reduced by 30, 40, 31, 43, 65 and 31 % for **2** and **4–8** respectively. Noticeably, **7** was much more active than **8**, quite the reverse than previously observed for Il-6 and Tnf-α, suggesting that the OAc group on C-5 (PAF **8**) is detrimental to the activity on this target (Fig. 1).

The phosphorylation of p38MAPK, ERK, JNK, the main regulators of inflammatory pathways was performed using the specific phosphorylated antibodies p38 Thr180/Tyr182, pERK Thr202/Tyr204 and pJNK Thr183/Tyr185. We first validated that, in our experimental conditions, LPS treatment induces the activation of p38, ERK and JNK signaling pathways (Fig. 6A and C-E). The p38MAPK pathway was the most affected by the tested flavones (Fig. 6A and E). Indeed, they all significantly decreased p38 activation in control conditions but also strongly diminished p38 activation under LPS by 59 (**2**), 69 (**4**), 49 (**5**), 46 (**6**), 80 (**7**) and 64 % (**8**). Concerning the JNK pathway, they showed no effects under basal conditions (data not shown). Upon LPS treatment, **2** and **5** were not efficient while **4**, **6**, **7** and **8** significantly reduced JNK activation by 57, 89, 89, and 81 %, respectively (Fig. 6A and D). None of the

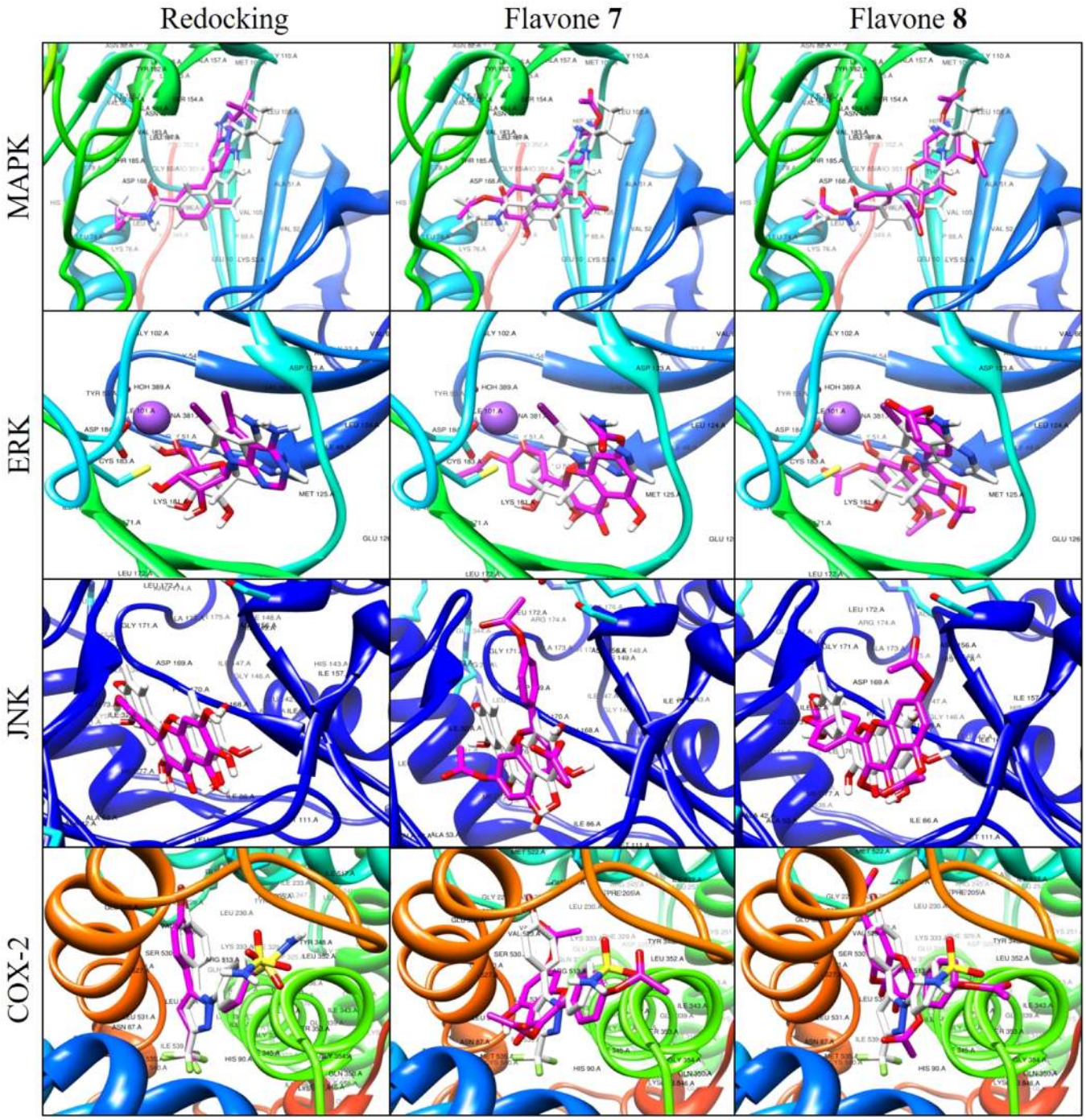

Fig. 7. Best poses after dockings, showing the co-crystallized ligand (Redocking, first column), and flavones **7** and **8**, within the four targets (*First column:* in white, native conformations of the co-crystallized ligands; in magenta, conformation after redocking. *Second and third columns:* in white, the co-crystallized ligands; in magenta, the flavone derivative docked).

compounds showed effects on the ERK pathway in unstimulated conditions (data not shown) or upon LPS treatment (Fig. 6A and C).

Concerning **1** (viscosine), *in vivo* effects have been previously observed at 30 mg/kg [30]. Here, we comforted these data *in vivo* at 10 mg/kg but we were not able to detect anti-inflammatory activity *in vitro*. This is also the case for santin (**2**). Indeed, anti-inflammatory activities of **2** have been described *in vitro* involving p38, JNK and ERK pathways in influenza-infected THP-1 cells at 60 μM (Zhong et al., 2019). Here at 10 μM, we only detected a downregulation of p38 phosphorylation. These results clearly underlined the importance of the concentration of the tested molecules and the models used. In any case, our results highlighted the potency of PMFs/PAFs derivatives to drop inflammation through controlling MAPK signaling pathway, in particular JNK and p38 by **7** and **8**.

3.3. Molecular docking study

Finally, a docking study was performed aiming to corroborate the involvement of the pre-selected targets in the anti-nociceptive effects of the tested compounds. Table 1 shows the values of binding energy (BE, Kcal/mol) and RMSD (Root Mean Square Deviation) of redocking procedures, as well as the BE for all the derivatives. They were all able to

find a geometry orientation relatively stable on the binding site of MAPK, ERK, JNK and COX-2. First, the results clearly demonstrate that PAFs **7** and **8** exhibited the best BE to all targets (Table 1, in bold), which surely explains their beneficial effects in both acetic-acid-writhing-induced nociception test and formalin test (especially on the second phase) and their efficacy *in vitro*. At the molecular level, the acetyl groups seem to provide more interaction points on binding sites and consequently a better BE than in the case of rhamnetin for example [35], reflecting a stronger inhibition and thus a better activity. To illustrate these observations, a visual perspective for the complexes involving **7** and **8** besides the co-crystallized ligands within the four targets is given (Fig. 7). Together, these *in silico* data reinforced the hypothesis that the mechanism of action of these two PAFs may involve, at least partially, the modulation of the MAPK inflammatory signaling pathways and thus probably the decrease the production of inflammatory mediators.

Considering the other active derivatives in the acetic acid test, flavone **2**, which had a similar profile to **8** in the formalin test, as well as **1,** demonstrated a good *in silico* profile with ERK and COX-2. On the contrary, compound **3**, less active in peripheral profile, showed the worst interaction energy with ERK among other targets. Compounds **4**, **5** and **6** behave the same way: **4** exhibited better BE with COX-2, while **5** showed better BE with COX-2 and JNK, **6** had stronger interactions with JNK and MAPK. These properties may probably contribute to their *in vivo* activity, though they had equally weaker interactions on ERK (Table 1). These data partially corroborate the previous WB's data on **5** where it seems to dampen COX-2 but not JNK phosphorylation levels, quite the reverse to **4** and **6** which both interfere with the levels of COX-2, JNK and p38 phosphorylation. These data reinforce the idea that **1**-**6** might interact with key inflammatory kinases or enzyme and potentially interfere with and thus probably inhibit their activities in a concentration dependent manner. Although our findings indicate that the compounds likely modulate the JNK and p38 pathways, further detailed studies are ongoing to conclusively elucidate the precise mechanisms involved.

4. Conclusion

A library of PMFs and PAFs was evaluated on several *in vivo* models of nociception and *in vitro* aiming to determine their anti-inflammatory capacities. The role of the substitution pattern was examined and compounds **5**, **7** and **8** were found the most active. A peripheral anti-nociceptive profile was demonstrated, indicating that they probably interfere with inflammatory pathways usually involved in pain disorders. These data were confirmed by monitoring anti-inflammatory activities and were corroborated with a molecular docking analysis, showing favorable interactions with targets attributed in the literature to flavonoids *i.e.,* MAPK and COX-2 proteins. The PAFs **7** and **8** showed the best binding energies, suggesting the role of a higher molecular volume in the affinity of these analogs. These compounds were the most efficient for tackling inflammation, probably by interfering with JNK and p38 pathways. Overall, these results pave the way for lead optimizations through further pharmacomodulation and design of new analgesic and anti-inflammatory drugs.

CRediT authorship contribution statement

Lucindo José Quintans Júnior: Writing – review & editing, Resources. **Jackson Roberto Guedes da Silva Almeida:** Writing – review & editing, Validation, Resources. **Sammya Yasmin Evangelista Mendes de Lima:** Investigation, Data curation. **Vincent Dumontet:** Resources. **Raimundo Gonçalves de Oliveira Júnior:** Writing – original draft, Validation, Supervision, Project administration, Methodology, Investigation, Formal analysis, Data curation, Conceptualization. **Clément Daviaud:** Writing – original draft, Investigation, Formal analysis, Data curation. **Raphaël Grougnet:** Writing – review & editing, Supervision, Project administration, Conceptualization. **Laurent Picot:** Writing – review & editing, Validation, Resources. **Kévin Baranger:** Writing – original draft, Validation, Resources, Methodology, Investigation, Funding acquisition, Formal analysis, Conceptualization. **Christiane Adrielly Alves Ferraz:** Investigation, Formal analysis, Data curation. **Mariana Gama e Silva:** Investigation, Formal analysis, Data curation. **Edilson Beserra de Alencar Filho:** Writing – original draft, Validation, Methodology, Investigation, Data curation.

Declaration of Competing Interest

The authors declare that they have no known competing financial interests or personal relationships that could have appeared to influence the work reported in this paper.

Acknowledgments

The authors thank the North Province of New Caledonia for facilitation of field investigations, Cyril Poulain for assistance in plant collection and Chouaha Bouzidi for her technical role on compounds obtention. This work was supported by funding from the CNRS, La Rochelle Université, Ligue Contre le Cancer CD17, and by the French National Research Agency (ANR) HeparInfSkin (ANR-21-CE44–0004) project to KB. CD was recipient of a doctoral fellowship from La Rochelle Université. Finally, the authors thank the Franco-Brazilian Network on Natural Products (FB2NP: https://fb2np.univ-lr.fr/) for the scientific support.

References

[1] A.V. Apkarian, Definitions of nociception, pain, and chronic pain with implications regarding science and society, Neurosci. Lett. Press (2018) 0–1, https://doi.org/10.1016/j.neulet.2018.11.039.
[2] A. Bell, The neurobiology of acute pain, Vet. J. 237 (2018) 55–62, https://doi.org/10.1016/j.tvjl.2018.05.004.
[3] C.E. Steeds, The anatomy and physiology of pain, Surgery 34 (2016) 55–59, https://doi.org/10.1016/j.mpsur.2015.11.005.
[4] P. Dinakar, A.M. Stillman, Pathogenesis of pain, Semin. Pediatr. Neurol. 23 (2016) 201–208, https://doi.org/10.1016/j.spen.2016.10.003.
[5] S.M. Walker, Overview of neurodevelopment and pain research, possible treatment targets, Best Pract. Res. Clin. Rheumatol. 28 (2014) 213–228, https://doi.org/10.1016/j.berh.2014.03.007.
[6] R.P. Yezierski, P. Hansson, Inflammatory and neuropathic pain from bench to bedside: what went wrong? J. Pain. 19 (2018) 571–588, https://doi.org/10.1016/j.jpain.2017.12.261.
[7] K. Brune, P. Patrignani, New insights into the use of currently available non-steroidal anti-inflammatory drugs, J. Pain. Res. 8 (2015) 105–118.
[8] R. Benyamin, A.M. Trescot, S. Datta, R. Buenaventura, R. Adlaka, N. Sehgal, S. E. Glaser, R. Vallejo, Opioid complications and side effects, Pain. Physician 11 (2008) 105–120.
[9] K. Pandurangan, V. Krishnappan, V. Subramanian, Antinociceptive effect of certain dimethoxy flavones in mice, Eur. J. Pharmacol. 727 (2014) 148–157, https://doi.org/10.1016/j.ejphar.2014.01.033.
[10] K. Vidyalakshmi, P. Kamalakannan, S. Viswanathan, S. Ramaswamy, Antinociceptive effect of certain dihydroxy flavones in mice, Pharmacol. Biochem. Behav. 96 (2010) 1–6, https://doi.org/10.1016/j.pbb.2010.03.010.
[11] N. Xue, X. Wu, L. Wu, L. Li, F. Wang, Antinociceptive and anti-inflammatory effect of Naringenin in different nociceptive and inflammatory mice models, Life Sci. 217 (2019) 148–154, https://doi.org/10.1016/j.lfs.2018.11.013.
[12] Ü.D. Özkay, Ö.D. Can, Anti-nociceptive effect of vitexin mediated by the opioid system in mice, Pharmacol. Biochem Behav. 109 (2013) 23–30, https://doi.org/10.1016/j.pbb.2013.04.014.
[13] M.D. Santi, C. Bouzidi, N.S. Gorod, M. Puiatti, S. Michel, R. Grougnet, M.G. Ortega, In vitro biological evaluation and molecular docking studies of natural and semisynthetic flavones from Gardenia oudiepe (Rubiaceae) as tyrosinase inhibitors, Bioorg. Chem. 82 (2019) 241–245, https://doi.org/10.1016/j.bioorg.2018.10.034.
[14] L.H. Mai, G.G. Chabot, P. Grellier, L. Quentin, V. Dumontet, C. Poulain, L. S. Espindola, S. Michel, H.T.B. Vo, B. Deguin, R. Grougnet, Antivascular and anti-parasite activities of natural and hemisynthetic flavonoids from New Caledonian Gardenia species (Rubiaceae), Eur. J. Med. Chem. 93 (2015) 93–100, https://doi.org/10.1016/j.ejmech.2015.01.012.
[15] M.D. Santi, M.P. Zunini, B. Vera, C. Bouzidi, V. Dumontet, A. Abin-carriquiry, R. Grougnet, M.G. Ortega, Xanthine oxidase inhibitory activity of natural and hemisynthetic flavonoids from Gardenia oudiepe (Rubiaceae) in vitro and molecular docking studies, Eur. J. Med. Chem. 143 (2018) 577–582, https://doi.org/10.1016/j.ejmech.2017.11.071.

[16] M. Zimmermann, Ethical guidelines for investigations of experimental pain in conscious animals, Pain 16 (1983) 109–110, https://doi.org/10.1016/0304-3959(83)90201-4.
[17] R. Koster, M. Anderson, E.J. De Beer, Acetic acid for analgesic screening, Fed. Proc. 18 (1959) 412–417.
[18] S. Hunskaar, K. Hole, The formalin test in mice: dissociation between inflammatory and non-inflammatory pain, Pain 30 (1987) 103–104, https://doi.org/10.1016/0304-3959(87)90088-1.
[19] S. Zhang, X. Guan, W. Liu, Z. Zhu, H. Jin, Y. Zhu, Y. Chen, M. Zhang, C. Xu, X. Tang, J. Wang, W. Cheng, W. Lin, X. Ma, J. Chen, YTHDF1 alleviates sepsis by upregulating WWP1 to induce NLRP3 ubiquitination and inhibit caspase-1-dependent pyroptosis, Cell Death Discov. 8 (2022) 244, https://doi.org/10.1038/s41420-022-00872-2.
[20] N.C. Souza, E.N. de Oliveira Nascimento, I.B. de Oliveira, H.M.L. Oliveira, E.G. P. Santos, M.E.R. Moreira Cavalcanti Mata, D.P. Gelain, J.C.F. Moreira, R.J. S. Dalmolin, M.A. de Bittencourt Pasquali, Anti-inflammatory and antioxidant properties of blend formulated with compounds of Malpighia emarginata D.C (acerola) and Camellia sinensis L. (green tea) in lipopolysaccharide-stimulated RAW 264.7 macrophages, Biomed. Pharmacother. 128 (2020) 110277, https://doi.org/10.1016/j.biopha.2020.110277.
[21] L. Su, M. Athamna, Y. Wang, J. Wang, M. Freudenberg, T. Yue, J. Wang, E.M. Y. Moresco, H. He, T. Zor, B. Beutler, Sulfatides are endogenous ligands for the TLR4–MD-2 complex, Proc. Natl. Acad. Sci. USA 118 (2021), https://doi.org/10.1073/pnas.2105316118.
[22] D.B. Kitchen, H. Decornez, J.R. Furr, J. Bajorath, Docking and scoring in virtual screening for drug discovery: methods and applications, Nat. Rev. Drug Discov. 3 (2004) 935–949.
[23] E.F. Pettersen, T.D. Goddard, C.C. Huang, G.S. Couch, D.M. Greenblatt, E.C. Meng, T.E. Ferrin, UCSF Chimera - a visualization system for exploratory research and analysis, J. Comput. Chem. 25 (2004) 1605–1612.
[24] X.Y. Meng, H.X. Zhang, M. Mezei, M. Cui, Molecular docking: a powerful approach for structure-based drug discovery, Curr. Comput. Aided Drug Des. 7 (2011) 146–157, https://doi.org/10.2174/157340911795677602.
[25] M.F. Sanner, Python: a programming language for software integration and development, J. Mol. Graph Model 17 (1999) 57–61.
[26] G.M. Morris, R. Huey, W. Lindstrom, M.F. Sanner, R.K. Belew, D.S. Goodsell, A. J. Olson, AutoDock4 and AutoDockTools4: automated docking with selective receptor flexibility, J. Comput. Chem. 30 (2009) 2785–2791, https://doi.org/10.1002/jcc.21256.
[27] J.J.P. Stewart, Optimization of parameters for semiempirical methods I. Method, J. Comput. Chem. 10 (1989) 209–220, https://doi.org/10.1002/jcc.540100208.
[28] M.A.S. Coutinho, M.F. Muzitano, S.S. Costa, Flavonoids: potential therapeutic agents for the inflammatory process, Rev. Virtual De. Quím. 1 (2009) 241–256.
[29] V. Jacob, T. Haga, K. Soliman, Structure-activity relationships of flavonoids, Curr. Org. Chem. 15 (2011) 2641–2657.
[30] A. Muhammad, B. Khan, Z. Iqbal, A.Z. Khan, I. Khan, K. Khan, M. Alamzeb, N. Ahmad, K. Khan, S. Lal Badshah, A. Ullah, S. Muhammad, M.T. Jan, S. Nadeem, N. Kabir, Viscosine as a potent and safe antipyretic agent evaluated by yeast-induced pyrexia model and molecular docking studies, ACS Omega 4 (2019) 14188–14192, https://doi.org/10.1021/acsomega.9b01041.
[31] M. Zhong, H.-Q. Wang, H.-Y. Yan, S. Wu, Z.-Y. Gu, Y.-H. Li, Santin inhibits influenza A virus replication through regulating MAPKs and NF-κB pathways, J. Asian Nat. Prod. Res. 21 (2019) 1205–1214, https://doi.org/10.1080/10286020.2018.1520221.
[32] S. Gorzalczany, M.A. Rosella, E.D. Spegazzini, C. Acevedo, S.L. Debenedetti, Anti-inflammatory activity of Heterotheca subaxillaris var. latifolia (Buckley) Gandhi & R.D. Thomas, Asteraceae, Rev. Bras. De. Farmacogn. 19 (2009) 876–879, https://doi.org/10.1590/S0102-695X2009000600014.
[33] W.A. Verri-Junior, F.T.M.C. Vicentini, M.M. Baracat, S.R. Georgetti, R.D. R. Cardoso, T.M. Cunha, S.H. Ferreira, F.Q. Cunha, M.J.V. Fonseca, R. Casagrande, Chapter 9 - Flavonoids as anti-inflammatory and analgesic drugs: mechanisms of action and perspectives in the development of pharmaceutical forms, Stud. Nat. Prod. Chem. (2012) 297–330.
[34] M. Cargnello, P.P. Roux, Activation and function of the MAPKs and their substrates, the MAPK-activated protein kinases, Microbiol. Mol. Biol. Rev. 75 (2011) 50–83, https://doi.org/10.1128/MMBR.00031-10.
[35] H.N. Jnawali, E. Lee, K.W. Jeong, A. Shin, Y.S. Heo, Y. Kim, Anti-inflammatory activity of rhamnetin and a model of its binding to c-Jun NH2-terminal kinase 1 and p38 MAPK, J. Nat. Prod. 77 (2014) 258–263, https://doi.org/10.1021/np400803n.